

1
2
3
4
5
6
7
8
9
10
11
12
13
14 **Effects of Ionic Concentration Gradient on**
15
16
17 **Electroosmotic Flow Mixing in a Microchannel**
18
19
20
21
22

23
24 Ran Peng and Dongqing Li*
25
26
27

28 Department of Mechanical and Mechatronics Engineering
29

30 University of Waterloo
31

32 Waterloo, Ontario, Canada N2L 3G1
33
34
35
36
37
38
39
40
41
42
43
44
45

46 *Corresponding author, Address: 200 University Ave. West, Waterloo, Ontario, N2L 3G1
47

48 Email: dongqing@uwaterloo.ca (D. Li)
49

50 Tel: +1 519-888-4567 x38682
51
52
53

54 The final publication is available at Elsevier via <http://dx.doi.org/10.1016/j.jcis.2014.10.061>. © 2014. This manuscript version
55 is made available under the CC-BY-NC-ND 4.0 license <http://creativecommons.org/licenses/by-nc-nd/4.0/>
56
57
58
59
60
61

1
2
3
4 **Abstract**
5

6
7 Effects of ionic concentration gradient on electroosmotic flow (EOF) mixing of one stream
8 of a high concentration electrolyte solution with a stream of a low concentration electrolyte
9 solution in a micrichannel are investigated numerically. The concentration field, flow field and
10 electric field are strongly coupled via concentration dependent zeta potential, dielectric constant
11 and electric conductivity. The results show that the electric field and the flow velocity are non-
12 uniform when the concentration dependence of these parameters is taken into consideration. It is
13 also found that when the ionic concentration of the electrolyte solution is higher than 1M, the
14 electrolyte solution essentially cannot enter the channel due to the extremely low electroosmotic
15 flow mobility. The effects of the concentration dependence of zeta potential, dielectric constant
16 and electric conductivity on electroosmotic flow mixing are studied.
17
18
19
20
21
22
23
24
25
26
27

28 **Key Words:** Flow mixing, Electroosmotic flow, Ionic concentration, Zeta potential, Dielectric
29 constant
30
31
32
33
34
35
36
37
38
39
40
41
42
43
44
45
46
47
48
49
50
51
52
53
54
55
56

57 Abbreviation: EOF, electroosmotic flow
58 ICEKF, induced-charge electrokinetic flow
59 EDL, electrical double layer
60
61

1
2
3
4 **1. Introduction**
5

6 Flow mixing in microchannels is an essential step for realizing biological and chemical
7 reactions in lab-on-a-chip devices [1]. Electroosmotic flow (EOF), as an excellent transport
8 method, has been widely used to pump chemical and biological reagents in microchannels
9 because of its significant advantages over pressure-driving flow, i.e., easy to control, plug-like
10 velocity profile and no mechanical moving parts. Electroosmotic flow based mixing is also
11 widely used in microfluidic systems. Generally, electroosmotic flow based mixing can be
12 categorized as laminar flow mixing and chaotic mixing [2]. In laminar flow mixing, flow
13 velocity is low, no turbulence exists in the system, and the mixing of two liquid streams in the
14 microchannel mainly depends on molecular diffusion. In the case of chaotic EOF mixing, the
15 vortices generated by the electrical field induced electroosmotic flow are used to enhance the
16 mixing.
17
18
19
20
21
22
23
24
25

26 A variety of experimental and theoretical research has been done to study the mixing
27 process in microfluidic systems. Most of them focused on enhancing the efficiency of mixing by
28 passive or active methods. For passive mixers, complex channel geometries were used to
29 increase the interaction area between the mixing liquids to achieve complete mixing within a
30 short transport distance [3]–[6]. On the other hand, active mixing methods introduce external
31 energy sources into the mixing process to enhance the mixing efficiency [6] [7]. Using variable
32 zeta potentials, Erickson [8] introduced oppositely charged surface patches into the microchannel,
33 and obtained localized flow circulations to enhance the mixing. Glasgow and Lin [9][10]
34 designed T-form EOF mixers and switched EOF alternatively by changing the electrical field
35 periodically to control the flow rates of the two streams to enhance mixing. Lin [11] studied
36 EOF mixing by controlling a gradient distribution of zeta potential by changing the frequency
37 of electric power applied on the shielding electrodes along the channel walls. Induced-charge
38 electrokinetic flow (ICEKF) is also a novel method to enhance the mixing efficiency and to
39 control the flow rate by controlling the vortices of the induced charge electroosmotic flow[12]–
40 [14]. It should be noted that all these works reported in the literature did not consider the ionic
41 concentration effects on both the EOF and EOF flow mixing process.
42
43
44
45
46
47
48
49
50
51
52
53
54
55

56 The ionic concentrations of most buffer solutions used in microfluidic systems are higher
57 than 10 mM, giving rise to a thin electrical double layer (EDL) with a thickness on the order of
58
59
60
61

1
2
3
4 10 nm. For thin EDL, the velocity of the EOF can be calculated from the Helmholtz-
5 Smoluchowski equation[15]:
6

$$\vec{V}_{EOF} = \varepsilon \zeta \vec{E} / \eta, \quad (1)$$

7
8
9
10
11 where ε is the local dielectric constant, ζ is the zeta potential of the solid boundary, η is the
12 viscosity of the solution and \vec{E} is the external electric field. All these parameters contribute to the
13 EOF velocity and hence affect EOF flow mixing. It should be realized that the ionic
14 concentration will directly affect the dielectric constant and the electrical conductivity of the
15 electrolyte solution, as well as the zeta potential. However, the dependence of these parameters
16 on the ionic concentration was not considered in previous studies of EOF flow mixing.
17
18
19
20
21
22

23 In this work, the ionic concentration effects on electroosmotic flow and the EOF flow
24 mixing were investigated. A finite element numerical model was developed to study the ionic
25 concentration effects on electroosmotic flow mixing in a straight microchannel. Concentration
26 dependent zeta potential, dielectric constant and electrical conductivity were used in the model,
27 which makes the electric field, the concentration field and the flow field fully coupled. The
28 influences of ionic concentration on electroosmotic flow mixing are discussed especially for very
29 high concentration difference between the two mixing streams.
30
31
32
33
34
35
36
37
38

39 2. Physical and mathematical models

40
41 Figure 1 shows the top-view of the simplified flow-mixing system to be modeled in this
42 work, two streams of different electrolyte solutions entering a straight microchannel under an
43 applied electrical potential difference, V_1 at the entrance of the channel and V_2 at the exit. For
44 simplicity, the electrolyte solutions are considered as aqueous NaCl solutions. The two streams
45 of NaCl solutions have different concentrations (C_1 and C_2 , respectively). The microchannel is
46 $200\mu m$ in width, $50\mu m$ in depth and $2mm$ in length. The channel walls are made of glass.
47 Because there is no concentration gradient in the channel depth direction, and the identical top
48 and bottom channel walls will not affect the EOF in the width and length directions, this system
49 can be simplified as a 2-D model as shown in Figure 1 and this treatment will not affect the
50 conclusions on EOF flow mixing of this paper.
51
52
53
54
55
56
57
58
59
60
61
62
63
64
65

2.1 Governing equations and boundary conditions

2.1.1 Electric field

The walls of the glass microchannel are electrically non-conducting. The electric current conversation in the channel must be satisfied, that is

$$\nabla \hat{i} = 0, \quad (2)$$

where \hat{i} is the current in the microchannel and can be written as

$$\hat{i} = \lambda(c)\vec{E}. \quad (3)$$

In the above equation, $\lambda(c)$ is the electric conductivity and a function of ionic concentration; the electric field, \vec{E} , can be calculated by the electric potential φ gradient:

$$\vec{E} = -\nabla\varphi \quad (4)$$

Combing equation (2) to (4), the electric field in the channel can be described by

$$\nabla(-\lambda(c)\nabla\varphi) = 0. \quad (5)$$

The boundary conditions of the electric field are given by:

$$\hat{n}\nabla\varphi = 0 \text{ at the channel walls ;} \quad (6a)$$

$$\varphi = V_1 \text{ at the inlet ;} \quad (6b)$$

$$\varphi = V_2 = 0 \text{ at the exit.} \quad (6c)$$

2.1.2 Flow field

As the electroosmotic flow of the aqueous electrolyte solutions is an incompressible laminar flow, the flow field can be calculated by Navier-Stokes equation and the continuity equation as follows[16]:

$$\rho \left[\frac{\partial \vec{u}}{\partial t} + \vec{u}\nabla\vec{u} \right] = -\nabla P + \mu\nabla^2\vec{u} + \vec{E}\rho_e - \frac{1}{2}\vec{E}^2\nabla\epsilon, \quad (7a)$$

$$\nabla \cdot \vec{u} = 0 \quad (7b)$$

where ρ is the density of the solution, t is the time, \vec{u} is the velocity vector, μ is the viscosity, ∇P is the pressure gradient. ρ_e is the net charge density and $\vec{E} = -\nabla\varphi$ is the applied electrical field.

The third term on the right hand side is the Coulomb force term due to the net charge, and the last term on the right hand side presents the dielectric force term due to the existence of dielectric permittivity gradient. Net charge can be generated in the bulk solution due to electric field and conductivity gradient, leading to electrohydrodynamic flow instabilities in microchannels [17]–[19]. Dielectric force can also contribute to the instabilities. However, one essential condition for the instabilities is that the electric field should be very high [18]. In this work, only low electric field situation is considered and we assume that instabilities will not occur. Consequently, the Coulomb force term and the dielectric force term in the bulk liquid phase are considered negligible.

Because the local net charge density is not zero only in EDL and the thickness of the EDL is considered sufficiently thin, the driving force term $\vec{E}\rho_e$ in Navier-Stokes equation can be neglected and the Helmholtz-Smoluchowski slip flow boundary is applied to account for the electroosmotic flow:

$$\vec{u} = -\frac{\varepsilon_0 \varepsilon_r(c) \zeta(c)}{\mu} \vec{E} \quad \text{at channel walls,} \quad (8)$$

where ε_0 is the permittivity in vacuum, $\varepsilon_r(c)$ is the relative dielectric constant, and $\zeta(c)$ is the zeta potential. Both $\varepsilon_r(c)$ and $\zeta(c)$ are functions of ionic concentration.

Considering a steady state electroosmotic flow without pressure difference along the channel, it follows:

$$P = 0 \quad \text{at the inlets and the exit.} \quad (9a)$$

Also, the pressure gradient is set to be zero at the channel walls:

$$\hat{n}\nabla P = 0 \quad \text{at channel walls.} \quad (9b)$$

2.1.3 Concentration field

According to the ionic transport theory [20], the concentration distribution can be described by

$$\frac{\partial C_i}{\partial t} = -\vec{u} \cdot \nabla C_i + D_i \nabla^2 C_i + \frac{z_i F D_i}{RT} (\nabla \cdot C_i \nabla \varphi) + R_i, \quad (10a)$$

C_i is the concentration of i th species, D_i is the diffusion coefficient of i th ion, z_i is the valence of i th ion, F is the Faraday constant, $F = eN_A$, where N_A is the Avogadro constant and e is the electronic charge; R is the gas constant, $R = k_b N_A$, where k_b is the Boltzmann constant; T is the temperature. R_i is the production rate due to chemical reactions. The term on the left hand side of this equation represents the accumulation rate of the ions. The terms on the right hand side of the equation stands for the contributions of convection, diffusion and migration in the mass transfer; the last term R_i on the right hand side is the production rate due to chemical reactions.

For steady state without chemical reactions, the accumulation rate term and the production rate due to chemical reactions can be deleted from the equation. Therefore, the governing equation for the concentration field is simplified as

$$\vec{u} \cdot \nabla C_i - D_i \nabla^2 C_i - \frac{z_i F D_i}{RT} (\nabla \cdot C_i \nabla \phi) = 0, \quad (10b)$$

For the electrolyte (containing Na^+ and Cl^-) considered in this study, the boundary conditions are

$$C = C_1 \text{ for stream 1 at the inlet,} \quad (11a)$$

$$C = C_2 \text{ for stream 2 at the inlet,} \quad (11b)$$

$$-\hat{n} N_i = 0 \text{ at channel walls, } N_i \text{ is the molar flux of } Na^+ \text{ and } Cl^-. \quad (11c)$$

2.2 Concentration dependent parameters

2.2.1 Zeta potential

A linear relationship between zeta potential and ionic concentration over a wide range of concentration for glass and silica material is given by [21] [22]

$$\zeta(c) = a_0 + a_1 pC, \quad (12)$$

where a_0 and a_1 are functions of temperature, pH, substrate material, and counterion type, pC is defined as $-\log_{10} \sum_i C_i$, where C_i are the ionic concentrations. a_0 is approximately zero for sodium and potassium solutions. Revil [23], [24] gives a_1 about -20mV for K^+ and Na^+ ions at $\text{pH}=7$. Therefore, the equation can be rewritten as

$$\zeta(c) = 20 \log_{10}(C_{Na^+} + C_{H^+}). \quad (10^{-6}M < C_{Na^+} < 1M) \quad (13a)$$

For pH = 7 solutions, because C_{H^+} (about $10^{-7}M$) is much smaller than C_{Na^+} and can be neglected when C_{Na^+} is more than $10^{-6}M$, the above equation is reduced to

$$\zeta(c) = 20 \log_{10}(C_{Na^+}) \text{ mV}. \quad (10^{-6}M < C_{Na^+} < 1M) \quad (13b)$$

In practice, when the ionic concentration is sufficiently high, for example, above 1M, the surface charge is essentially neutralized and EDL is negligible. Therefore, the zeta potential is considered to be zero when the ionic concentration is above 1M,

$$\zeta(c) = 0 \quad (C_{Na^+} > 1M). \quad (13c)$$

2.2.2 Dielectric constant

Peyman [25] measured the relative dielectric constant of NaCl solution from 0.001 mol/L to 5mol/L at 5°C ~ 35°C. Models and equations were developed to calculate the dielectric constant as a function of temperature and concentration. A curve-fitting function is given by:

$$\begin{aligned} \varepsilon_r(c) = \varepsilon_w(1 - 3.742 \times 10^{-4}TC + 0.034C^2 \\ - 0.178C + 1.515 \times 10^{-4}T - 4.929 \times 10^{-6}T^2), \end{aligned} \quad (14)$$

where T is the temperature of liquid (°C), C is the ionic concentration of the solution in mol/L. ε_w is the relative dielectric constant of water at the given temperature. This equation can be used to calculate the relative dielectric constant according to the local concentration. In this study, we use the mean concentration \bar{C} to calculate the dielectric constant, where

$$\bar{C} = \frac{C_{Na^+} + C_{Cl^-}}{2}. \quad (15)$$

2.2.3 Electrical conductivity

Electrical conductivity of the electrolyte solution is the most important factor to calculate the electric field. The electrical conductivity is proportional to the local ionic concentration. A non-uniform distribution of the electrical conductivity will make the electrical field non-uniform and in turn affect the EOF velocity field.

1
2
3
4 The electrical conductivity of aqueous electrolyte solutions mainly depends on the ionic
5 concentration. For a single salt electrolyte such as NaCl [20], the electric conductivity is given
6 by
7
8

$$\lambda(c) = \lambda_{Na^+}C_{Na^+} + \lambda_{Cl^-}C_{Cl^-}, \quad (16)$$

9
10
11
12 And at 25°C,

$$\lambda_{Na^+} = 5.01 * 10^{-3} Sm^2/mol \quad (17a)$$

13
14
15
16 and

$$\lambda_{Cl^-} = 7.63 * 10^{-3} Sm^2/mol . \quad (17b)$$

17
18
19
20 Therefore, the electrical conductivity of NaCl solution can be expressed as

$$\lambda(c) = (5.01C_{Na^+} + 7.63 C_{Cl^-}) * 10^{-3} S/m. \quad (18)$$

21 22 23 24 25 26 27 28 29 30 **2.3 Numerical method and parameter setting**

31 The above equations and boundary conditions were solved by using COMSOL 4.3b. The
32 number of the meshed triangle elements was 3863 and the boundary element was 478, in order to
33 achieve mesh independent results. A non-uniform grid refinement was generated at the entrance
34 and exit of the channel as well as at the channel walls.
35
36
37
38

39 In order to study the effects of the ionic concentration and the electric field strength on the
40 EOF velocity field and the flow mixing the numerical simulations were conducted under
41 different concentrations and electric field strengths. The concentration field, the electrical field,
42 the zeta potential, the dielectric constant and the electrical conductivity in the microchannel are
43 analyzed. Table 1 shows the parameters used in the simulation.
44
45
46
47
48
49
50
51

52 **3. Results and discussion**

53 **3.1 Two models**

54 In this part, two models were studied, one model where the dielectric constant, zeta potential
55 and the electric conductivity vary with the ionic concentration (called the variable model), and
56 another model where these parameters are constant (called the constant model). The results of
57
58
59
60
61
62
63
64
65

1
2
3
4 these two models are compared to show the differences in concentration field, electric field and
5 velocity field. In the constant model, the relative dielectric constant of pure water is set to be 78
6 at 25°C, the zeta potential of the glass-water interface takes the value of -62.6mV as measured
7 by Gu and Li [26]. The electric conductivity of pure water is $0.055\mu\text{S}/\text{cm}$. Table 2 shows the
8 dielectric constant, zeta potential and conductivity for the two models. Moreover, in both models,
9 the ionic concentrations of NaCl at the channel inlet are 0.1M for stream 1 and 10^{-6}M for
10 stream 2, respectively. The externally applied electric field is given by the following: 20V
11 electric potential is applied at the entrance of channel and the exit of the channel is set to be
12 ground (0V).
13
14
15
16
17
18
19
20
21
22

23 **3.2 Concentration field**

24
25
26 For the above-described models, the flow mixing of two streams of NaCl solutions was
27 studied. The concentration of NaCl at the entrance is 0.1M for stream 1 and 10^{-6}M for stream 2,
28 respectively. The externally applied electric field is 100V/cm. Figure 2 shows the ionic
29 concentration distribution in both the constant model and the variable model. It is clear that the
30 concentration at the exit region of the microchannel is much higher in the constant model (about
31 $50\text{mol}/\text{m}^3$) than that in the variable model ($25\text{mol}/\text{m}^3$). Furthermore, the ionic concentration
32 distribution in the constant model is essentially symmetrical in the channel width direction,
33 which means that the flow rates of stream 1 and stream 2 are equal. By contrast, in the variable
34 model, the high concentration can be observed only in a very small portion of the channel near
35 the entrance. This implies that a very small amount of the high concentration solution, stream 1,
36 enters the channel. Clearly, the constant model overestimated the flow mixing effect in
37 comparison with the variable model that considers the influences of the ionic concentration
38 distribution on the dielectric constant, zeta potential and electrical conductivity. How these
39 concentration dependent parameters affect the EOF mixing will be discussed further in the
40 following sections.
41
42
43
44
45
46
47
48
49
50
51
52
53
54
55
56
57
58
59
60
61
62
63
64
65

3.3 Influence of ionic concentration on electric conductivity, dielectric constant and zeta potential

Electric conductivity

As shown by Eq. (18), the electric conductivity increases with the ionic concentration. If the concentration of stream 1 is 0.1M, the electric conductivity of stream 1 at the channel entrance is about 1.36S/m. If the concentration of stream 2 is 10^{-6} M, the electric conductivity of stream 2 at the channel entrance is approximately 13.6 μ S/m. Clearly, there is a large difference in the electric conductivity between the stream 1 and the stream 2. Consequently, the concentration dependence of the electric conductivity will lead to a non-uniform distribution of electrical potential in the channel. It should also be noted that, in addition to the ionic concentration, different types of electrolytes and the ionic valence will have significant effects on the electric conductivity of the electrolyte solution.

Dielectric constant

As discussed before, the relative dielectric constant is a function of the ionic concentration as shown by Eq. (14). Figure 3 shows the dielectric constant distribution along the channel wall on the stream 1 side ($C_1 = 0.1$ M), and along the channel wall on the stream 2 side ($C_2 = 10^{-6}$ M). Dielectric constant near the channel wall on the stream 2 side is higher than that near the channel wall on the stream 1 side, because the ionic concentration of the stream 2 is lower. The biggest difference appears at the entrance region, 78 versus 76.6. That is, there is a 1.8% decrease in dielectric constant for 0.1M NaCl solution when compared with 10^{-6} M NaCl solution. Although such a small difference in this case may be neglected, however, for higher concentration EOF mixing, the change in dielectric constant value may become significant and should not be neglected. For example, when the concentration of stream 1 increases to 1M, while the concentration of stream 2 is kept constant at $C_2 = 10^{-6}$ M, the dielectric constant of stream 1 will reduce by 14.1%; if the concentration of stream 1 increases to 5M, the dielectric constant of stream 1 will reduce by 43.6%. It is obvious that such a large change in dielectric constant has to be considered in high concentration EOF mixing, because the EOF velocity (Eq.(8)) is a linear function of the dielectric constant.

Zeta potential

As the ionic concentration varies along the microchannel during the flow mixing, zeta potential changes with the ionic concentration, as indicated by Eq. (13). The higher the ionic concentration, the lower zeta potential value. Figure 4 presents the zeta potential distribution along the channel walls. Because of the large concentration difference at the entrance, there is a huge zeta potential difference between the wall on stream 1 side and the wall on stream 2 side at the entrance. For the wall on stream 1 side at the entrance, the calculated zeta potential by Eq. (13b) is approximately -20 mV, in a good agreement with the measured values (-22.7 mV) as reported by Gu and Li [26]. For the channel wall on the stream 2 side, the calculated zeta potential by Eq. (13b) is approximately -120 mV at the entrance. As the solutions mix with the flow, the concentration on the stream 2 side increases, thus the value of zeta potential decreases rapidly and eventually reduced to -35 mV at the exit of the channel. On the other hand, zeta potential of the channel wall on stream 1 side increase slowly and reaches about -30 mV at the outlet region. As discussed before, when the local ionic concentration is higher than 1 M, zeta potential at that location is practically zero as described by Eq. (13c). Consequently there will be no electroosmotic flow at that location (Eq. (8)).

3.4 Electric field

Figure 5 presents the electric potential distributions in the constant model (Figure 5a) and the variable model (Figure 5b). As seen in this figure, in the constant model, the electric potential distribution is uniform and no electric field gradient exists in the channel width direction as indicated by the uniform electrical field lines. On the other hand, in the variable model, the electric field is non-uniform, especially at the entrance region. Based on the density of the electric field lines in the variable model, the electric field strength at the entrance of stream 1 is higher than anywhere else in the channel. Because the local electric conductivity of aqueous solution is proportional to the local ionic concentration, the higher ionic concentration of stream 1 at the entrance has a higher electric conductivity, and the lower ionic concentration of stream 2 at the entrance has a lower electric conductivity. This leads to the non-uniform electrical potential distribution as shown in Figure 5b for the variable model.

3.5 Flow field

Figure 6 describes the velocity vectors and streamlines in the entrance region of the channel in both the constant model (Figure 6a) and the variable model (Figure 6b). One can see that the flow velocity distribution in the constant model is uniform, approximately $430\mu\text{m/s}$; while in the variable model, the velocity is not uniform, and the local velocity decreases as the local concentration increases (see Figure 2) across the width direction of the channel. For the variable model, the highest velocity (about $825\mu\text{m/s}$) appears at the entrance on the stream 2 side channel wall where the local ionic concentration is the lowest. By contrast, the lowest velocity (about $100\mu\text{m/s}$) is located at the entrance of the channel wall of stream 1 side, where the ionic concentration is high and the zeta potential is low. At the exit region of the channel, the concentration distribution becomes more or less uniform and hence the velocity distribution approaches uniform. Clearly, the constant model overestimated the electroosmotic flow in comparison with the variable model.

3.6 Electroosmotic flow mixing of high concentration solutions

Based on the variable model, Figure 7 shows the velocity vectors and streamlines in the channel for two cases. In Figure 7(a), the ionic concentration of stream 1 is 5M, and in Figure 7(b), the ionic concentration of stream 1 is 1M. The applied electric field is 100V/cm in both cases. It is clear that the average velocity in the 1M model (Figure 7b) is higher than that in the 5M model (Figure 7a). From Eq. (8), we know that EOF velocity is proportional to zeta potential. As we discussed above, when the concentration is higher than 1M, zeta potential is nearly zero (Eq. (13c)). Consequently, EOF velocity near the channel wall on stream 1 side is extremely small and thus the stream 1 essentially cannot enter the channel. On the other hand, stream 2 has a much lower ionic concentration (10^{-6}M); the zeta potential and the EOF velocity are much higher on the channel wall on the stream 2 side. Therefore, the majority of the solution flowing into the channel is the more dilute solution, stream 2. This significantly impairs the desired results of the EOF mixing.

1
2
3
4 The EOF mixing for high ionic concentrations is also examined by the variable model that
5 considers the concentration dependence of electric conductivity, zeta potential and dielectric
6 constant. Figure 8 presents the dimensionless concentration distribution in the microchannel. In
7 these simulations, the concentration was nondimensionalized by $C^*=C/C_1$. Four different
8 concentrations of stream 1 (C_1), 5M, 1M, 0.1M, and 0.001M, were used respectively. The
9 applied electric field is 100V/cm. From Figure 8, one can see that the average concentrations C^*
10 at the channel exit in cases (a) and (b) are much lower (about 0.09 and 0.17, respectively) than
11 that in cases (c) and (d) (about 0.25 and 0.4, respectively). As discussed above, in the constant
12 model, the average concentrations C^* at the channel exit should be 0.5. In the variable model, i.e.,
13 when the effects of ionic concentration gradient are considered, very different mixing results
14 may appear. When the ionic concentration of stream 1 is too high, very little high concentration
15 solution can flow into the channel due to the nearly zero zeta potential at the entrance, resulting
16 in poor mixing efficiency.
17
18
19
20
21
22
23
24
25
26
27
28
29
30
31

32 4. Conclusion

33 A mathematical model was developed to consider the effects of ionic concentration on the
34 electroosmotic flow mixing of two streams of electrolyte solutions with different ionic
35 concentrations in a straight microchannel. The dependence of zeta potential, dielectric constant
36 and electric conductivity on ionic concentration was taken into account in this model. We found
37 that the ionic concentration difference between the mixing streams results in a non-uniform
38 electric field and a velocity gradient in the channel, especially at the entrance region. On the side
39 of the high concentration stream, zeta potential is small and electroosmotic flow mobility is low.
40 When the ionic concentration is close to 1M or higher, the solution of such a high concentration
41 essentially cannot enter the mixing channel by electroosmotic flow. Therefore, electroosmotic
42 flow mixing is not suitable for mixing one solution of a very high ionic concentration with
43 another low concentration solution. When studying the electroosmotic flow mixing of two
44 solutions with a large ionic concentration difference, the influence of the ionic concentration
45 should be considered. The model presented in this paper considers only low electrical field, and
46 hence the electroosmotic flow was assumed to be free of electrokinetic instabilities. Future study
47 may consider the concentration dependent variables, such as zeta potential, viscosity, dielectric
48
49
50
51
52
53
54
55
56
57
58
59
60
61
62
63
64
65

1
2
3
4 permittivity, conductivity, in the numerical simulation and compare the predictions with the
5
6 experimental results to investigate the electroknetic instability phenomena.
7
8
9

10 **Acknowledgements**

11
12
13
14 The authors wish to thank the financial support of the Natural Sciences and Engineering
15 Research Council (NSERC) of Canada through a research grant to Dr. Li.
16
17
18
19
20
21
22
23
24
25
26
27
28
29
30
31
32
33
34
35
36
37
38
39
40
41
42
43
44
45
46
47
48
49
50
51
52
53
54
55
56
57
58
59
60
61
62
63
64
65

References

- [1] D. Li, Ed., *Encyclopedia of Microfluidics and Nanofluidics*, First edit. New York: Springer, 2008.
- [2] C.-C. Chang and R.-J. Yang, “Electrokinetic mixing in microfluidic systems,” *Microfluid. Nanofluidics*, vol. 3, no. 5, pp. 501–525, Jun. 2007.
- [3] S. Naher, D. Orpen, D. Brabazon, C. R. Poulsen, and M. M. Morshed, “Effect of micro-channel geometry on fluid flow and mixing,” *Simul. Model. Pract. Theory*, vol. 19, no. 4, pp. 1088–1095, Apr. 2011.
- [4] V. Kumar, M. Paraschivoiu, and K. D. P. Nigam, “Single-phase fluid flow and mixing in microchannels,” *Chem. Eng. Sci.*, vol. 66, no. 7, pp. 1329–1373, Apr. 2011.
- [5] W. Jeon and C. B. Shin, “Design and simulation of passive mixing in microfluidic systems with geometric variations,” *Chem. Eng. J.*, vol. 152, no. 2–3, pp. 575–582, Oct. 2009.
- [6] V. Hessel, H. Löwe, and F. Schönfeld, “Micromixers—a review on passive and active mixing principles,” *Chem. Eng. Sci.*, vol. 60, pp. 2479–2501, 2005.
- [7] Y. K. Suh and S. Kang, “A Review on Mixing in Microfluidics,” *Micromachines*, vol. 1, no. 3, pp. 82–111, Sep. 2010.
- [8] D. Erickson and D. Li, “Influence of Surface Heterogeneity on Electrokinetically Driven Microfluidic Mixing,” *Langmuir*, vol. 18, no. 5, pp. 1883–1892, Mar. 2002.
- [9] C.-H. Lin, L.-M. Fu, and Y.-S. Chien, “Microfluidic T-form mixer utilizing switching electroosmotic flow.,” *Anal. Chem.*, vol. 76, no. 18, pp. 5265–72, Sep. 2004.
- [10] I. Glasgow, J. Batton, and N. Aubry, “Electroosmotic mixing in microchannels,” *Lab Chip*, vol. 4, no. 6, pp. 558–62, Dec. 2004.
- [11] J.-L. Lin, K.-H. Lee, and G.-B. Lee, “Active mixing inside microchannels utilizing dynamic variation of gradient zeta potentials.,” *Electrophoresis*, vol. 26, no. 24, pp. 4605–15, Dec. 2005.
- [12] Z. Wu and D. Li, “Mixing and flow regulating by induced-charge electrokinetic flow in a microchannel with a pair of conducting triangle hurdles,” *Microfluid. Nanofluidics*, vol. 5, no. 1, pp. 65–76, Sep. 2007.
- [13] F. Zhang, Y. Daghighi, and D. Li, “Control of flow rate and concentration in microchannel branches by induced-charge electrokinetic flow.,” *J. Colloid Interface Sci.*, vol. 364, no. 2, pp. 588–93, Dec. 2011.

- 1
2
3
4 [14] Z. Wu and D. Li, "Micromixing using induced-charge electrokinetic flow," *Electrochim. Acta*, vol. 53, no. 19, pp. 5827–5835, Aug. 2008.
5
6
7
8 [15] R. J. Hunter, *Zeta Potential in Colloid Science*. London: Academic Press, 1981.
9
10 [16] D. Saville, "Electrohydrodynamics: the Taylor-Melcher leaky dielectric model," *Annu. Rev. Fluid Mech.*, no. 1962, pp. 27–64, 1997.
11
12
13
14 [17] K. H. Kang, J. Park, I. S. Kang, and K. Y. Huh, "Initial growth of electrohydrodynamic instability of two-layered miscible fluids in T-shaped microchannels," *Int. J. Heat Mass Transf.*, vol. 49, no. 23–24, pp. 4577–4583, Nov. 2006.
15
16
17
18
19 [18] H. Lin, B. D. Storey, M. H. Oddy, C.-H. Chen, and J. G. Santiago, "Instability of electrokinetic microchannel flows with conductivity gradients," *Phys. Fluids*, vol. 16, no. 6, p. 1922, 2004.
20
21
22
23
24 [19] B. D. Storey, "Direct numerical simulation of electrohydrodynamic flow instabilities in microchannels," *Phys. D Nonlinear Phenom.*, vol. 211, no. 1–2, pp. 151–167, Nov. 2005.
25
26
27
28 [20] J. H. Masliyah and S. Bhattacharjee, *Electrokinetic and Colloid Transport Phenomena*. John Wiley & Sons, 2006.
29
30
31 [21] R. Hunter and H. Wright, "The dependence of electrokinetic potential on concentration of electrolyte," *J. Colloid Interface Sci.*, vol. 37, no. 3, pp. 564–580, 1971.
32
33
34
35 [22] B. J. Kirby and E. F. Hasselbrink, "Zeta potential of microfluidic substrates: 1. Theory, experimental techniques, and effects on separations.," *Electrophoresis*, vol. 25, no. 2, pp. 187–202, Jan. 2004.
36
37
38
39
40 [23] A. Revil and H. Schwaeger, "Streaming potential in porous media: 2. Theory and application to geothermal systems," *J. Geophys. Res.*, vol. 104, no. B9, pp. 20033–20048, 1999.
41
42
43
44
45 [24] a. Revil, P. a. Pezard, and P. W. J. Glover, "Streaming potential in porous media: 1. Theory of the zeta potential," *J. Geophys. Res.*, vol. 104, no. B9, p. 20021, 1999.
46
47
48
49 [25] A. Peyman, C. Gabriel, and E. H. Grant, "Complex permittivity of sodium chloride solutions at microwave frequencies.," *Bioelectromagnetics*, vol. 28, no. 4, pp. 264–74, May 2007.
50
51
52
53 [26] Y. Gu and D. Li, "The ζ -Potential of Glass Surface in Contact with Aqueous Solutions," *J. Colloid Interface Sci.*, vol. 226, no. 2, pp. 328–339, Jun. 2000.
54
55
56
57
58
59
60
61
62
63
64
65

List of figures

Figure 1 Schematic of the model flow-mixing system of two streams in a microchannel.

Figure 2 The ionic concentration distribution of the constant model (a) and the variable model (b). For both models, the concentration of NaCl at the entrance is 0.1M for stream 1 and 10^{-6} M for stream 2, respectively. The externally applied electric field is 100V/cm.

Figure 3 Relative dielectric constant distribution along the channel wall on the stream 1 side ($C1 = 0.1$ M) and along the channel wall on the stream 2 side ($C2=10^{-6}$ M), $E=100$ V/cm, $T = 25^{\circ}$ C.

Figure 4 Zeta potential distribution along the channel wall on the stream 1 side ($C1 = 0.1$ M) and along the channel wall on the stream 2 side ($C2= 10^{-6}$ M), $E=100$ V/cm, $T = 25^{\circ}$ C.

Figure 5 Electric potential distribution (V) and electric field lines in the constant model (a) and the variable model (b). For both models, the concentration of NaCl at the entrance is 0.1M for stream 1 and 10^{-6} M for stream 2, respectively. The externally applied electric field is 100V/cm, $T = 25^{\circ}$ C.

Figure 6 Velocity vectors and streamlines in the entrance region of channel in the constant model (a) and the variable model (b). For both models, the concentration of NaCl at the entrance is 0.1M for stream 1 and 10^{-6} M for stream 2, respectively. The externally applied electric field is 100V/cm.

Figure 7 Velocity vectors and streamlines in the channel. (a) At the entrance, the ionic concentration is 5M for stream 1 and 10^{-6} M for stream 2, respectively. (b) At the

entrance, the ionic concentration is 1M for stream 1 and 10^{-6} M for stream 2, respectively. The applied electric field is $E=100\text{V/cm}$ for both models.

Figure 8 Dimensionless concentration distribution in the microchannel ($C^*=C/C_1$). The ionic concentration of stream 1 is: (a) $C_1=5\text{M}$, (b) $C_1=1\text{M}$, (c) $C_1=0.1\text{M}$, (d) $C_1=0.001\text{M}$. The ionic concentration for stream 2 is 10^{-6}M for all cases. The applied electric field is 100V/cm in all these cases.

Figure 1

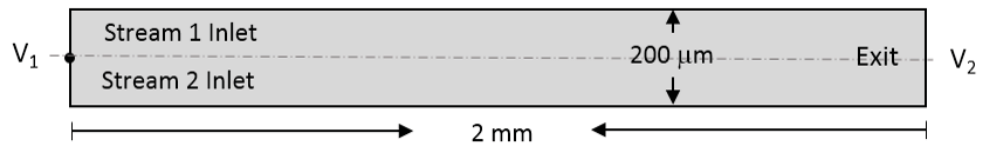


Figure 2

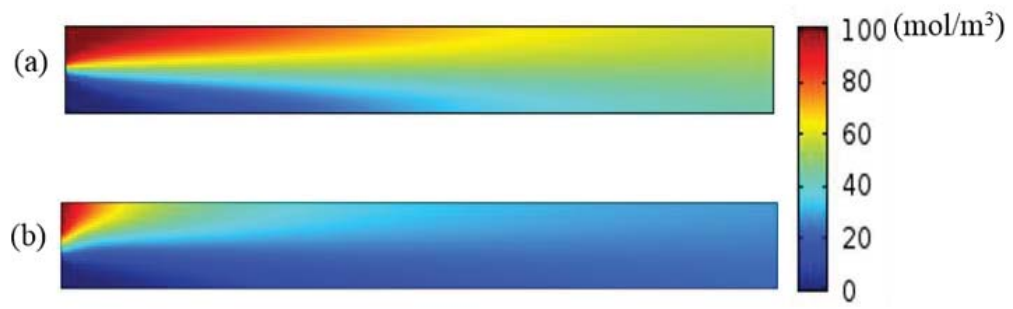


Figure 3

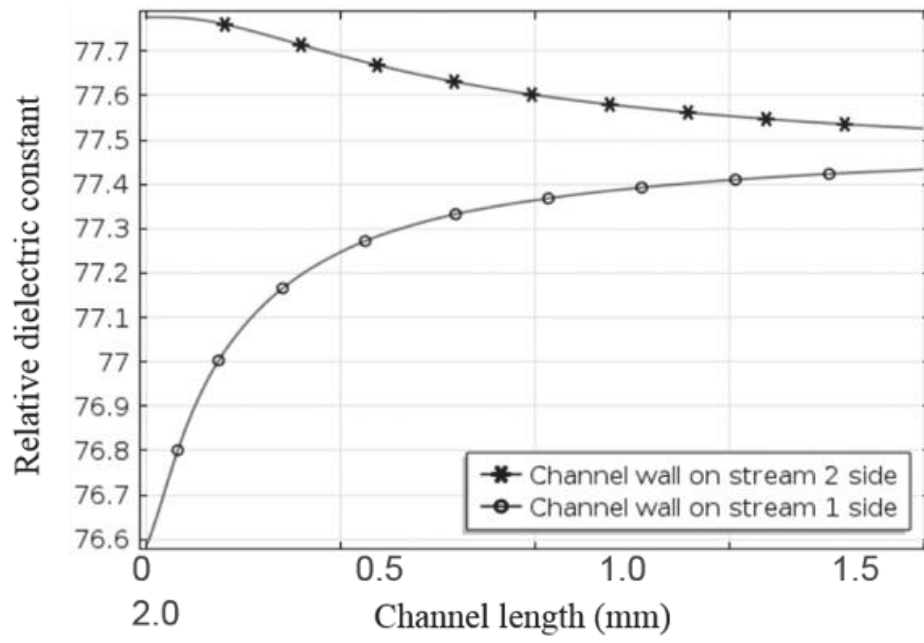


Figure 4

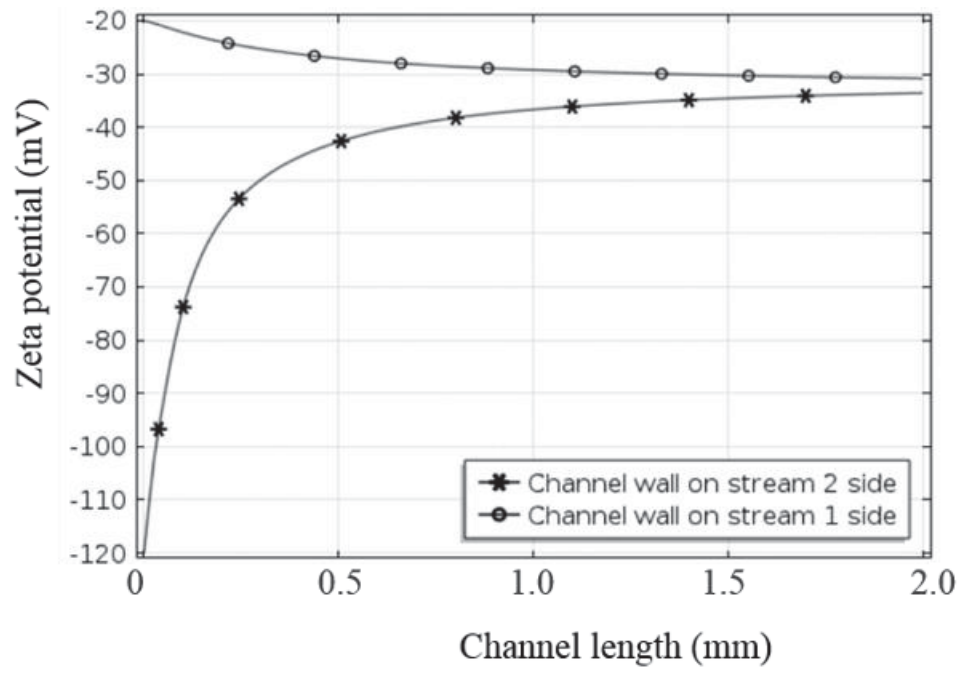


Figure 5

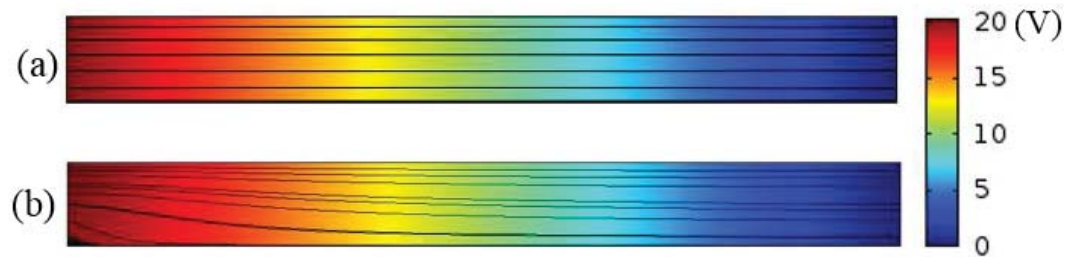


Figure 6

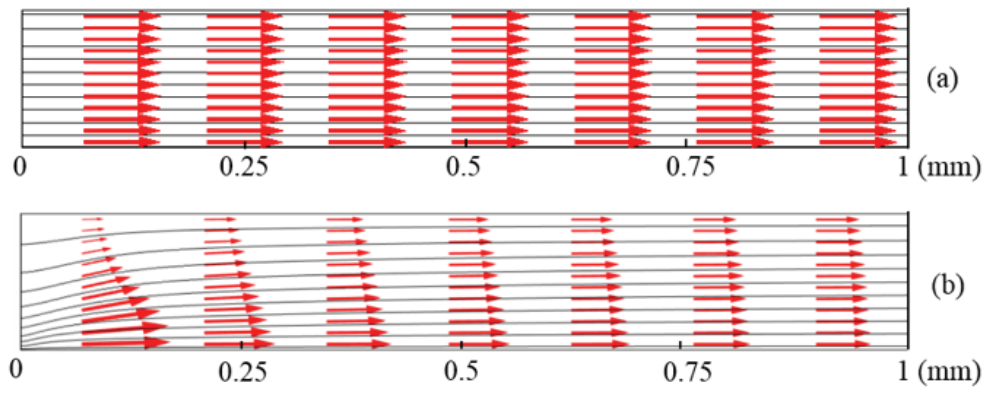


Figure 7

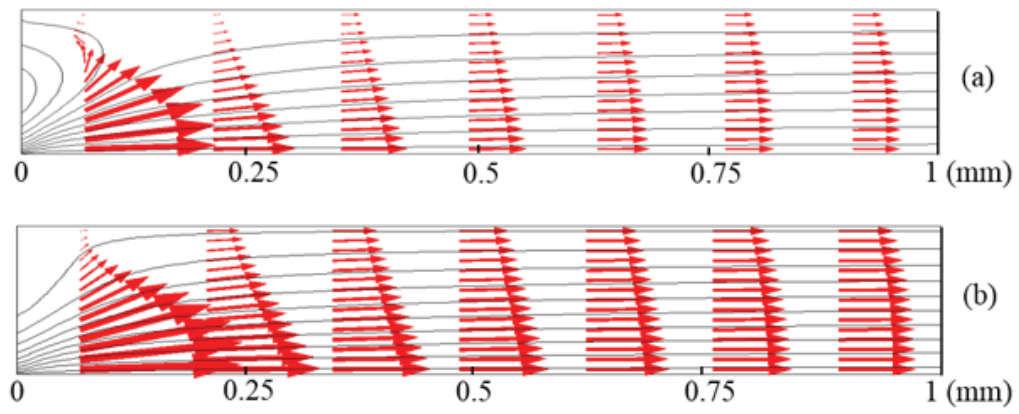
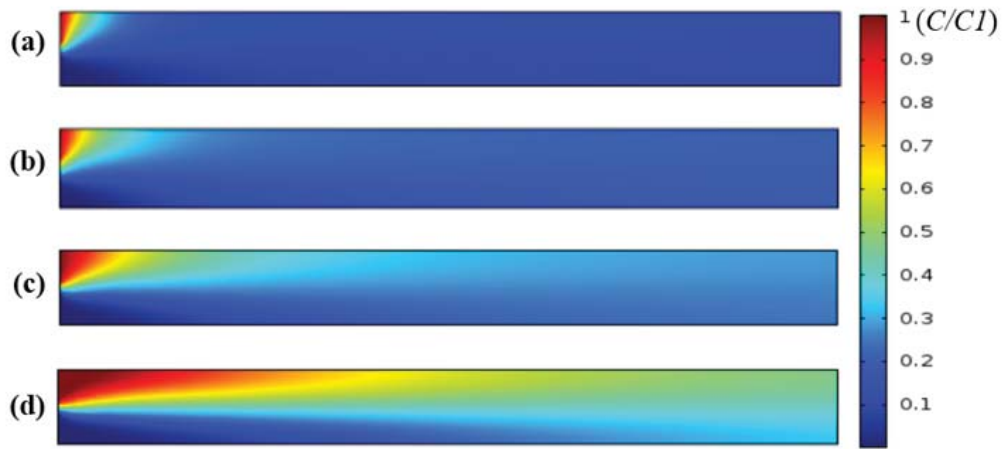


Figure 8



Tables

Table 1. Parameter values used in the simulation

Parameters	Value
Temperature	$T=25^{\circ}\text{C}$
Vacuum permittivity	$\epsilon_0 = 8.854 * 10^{-12}\text{F/m}$
Relative dielectric constant of water	$\epsilon_w = 78$
Density	$\rho = 998\text{kg/m}^3$
Dynamic viscosity	$\mu = 1.005 * 10^{-3}\text{Pa} \cdot \text{s}$
Diffusion coefficient of Na^+	$D_{\text{Na}^+} = 1.344 * 10^{-9}\text{m}^2/\text{s}$
Diffusion coefficient of Cl^-	$D_{\text{Cl}^-} = 2.03 * 10^{-9}\text{m}^2/\text{s}$
Valence of Na^+	$Z_{\text{Na}^+} = 1$
Valence of Cl^-	$Z_{\text{Cl}^-} = -1$
Faraday constant	$F=9.649*10^4\text{C/mol}$
Gas constant	$R=8.31\text{ J/mol/K}$
Concentration at inlet 2	$C_2 = 1 * 10^{-6}\text{mol/L}$

Table 2 Parameter setting for dependent models and constant model

Parameter \ Model	Variable model	Constant model
Dielectric constant (ϵ_r)	$\epsilon_r = \epsilon_r(c)$	$\epsilon_r = 78$
Zeta potential (ζ)	$\zeta = \zeta(c)$	$\zeta = -62.6mV$
Electric conductivity ($\lambda(c)$)	$\lambda = \lambda(c)$	$\lambda = 0.055\mu S/cm$
Electric field \vec{E}	$100V/cm$	